Nonprocessed Adipose Tissue Graft in the Treatment of Peri-Implant Osseous Defects in the Rabbit's Tibiae: A Pilot Study

Diogo Godoy Zanicotti, MS[1]*
Fernanda Brugin Matsubara, MS[2]
João César Zielak, PhD[2]
Allan Fernando Giovanini, PhD[2]
Cícero de Andrade Urban, PhD[2]
Tatiana Miranda Deliberador, PhD[2]

We hypothesized that a new technique using nonprocessed adipose tissue could regenerate bone around dental implants. Eighteen rabbits received 1 implant per tibia surrounded by a surgically created osseous defect. The defects were assigned for treatment into 3 groups: C, AT, and AB. The percentages of bone-to-implant contact were 17.64% ± 16.22% (AB), 3.54% ± 7.08% (AT), and 12.71% ± 10.11% (C) ($\rho = 0.25$). The use of adipose tissue around surgically created peri-implant osseous defects interferes with bone formation.

Key Words: dental implants, bone regeneration, adipose tissue, rabbits, tibia

INTRODUCTION

The placement of dental implants immediately after tooth extraction is being widely practiced nowadays. This procedure can reduce the total treatment time, since there is no need for a waiting period for implant placement postextraction. However, it may present a space between the crown portion of the implant and the surrounding alveolar bone. This space is commonly called a gap.

A great variety of bone grafts and/or biomaterials have been used to fill the gaps and improve the new bone formation.[1–3]

The search for new materials to help the process of bone regeneration around implants has yielded new ways that differ from those arising from the use of autogenous bone, allografts (allogenic bone), xenogenous bone (heterogeneous bone), biocermics, and bioactive glasses. Tissue engineering has been presented as one such way. Tissue engineering has significant potential in the development of organized and functional tissues. The foundation of any building tissue resulting from tissue engineering is the source of cells that will be used to start the new tissue grow.[4] One source of adult stem cells is the adipose tissue. This tissue presents an important reservoir of stem cells. The adipose-derived stem cells have the ability to differentiate into osteoblasts, with potential implications for human bone tissue engineering.[5,6] Moreover, adult subcutaneous unilocular adiposal cells present in vitro the capacity to dedifferentiate and then differentiate into osteoblasts (transdifferentiation).[7]

The aim of this study was to evaluate histologically the bone repair of surgically created peri-implant osseous defects (gaps) around titanium dental implants using a nonprocessed adipose tissue graft. The transdifferentiation capacity of adipocytes and the presence of adult stem cells in the adipose tissue may, hypothetically, promote

[1] University of Otago, Dunedin, New Zealand.
[2] Positivo University, Curitiba, Brazil.
* *Corresponding author,* e-mail: diogogz@hotmail.com
DOI: 10.1563/AAID-JOI-D-11-00149

bone repair without the need for adipose tissue–processing techniques.

Materials and Methods

The Ethics and Research Committee at Positivo University, Curitiba/PR, Brazil, approved this study protocol. All guidelines regarding the care of animal research subjects were strictly followed.

Animals

For the present study, 18 New Zealand white male rabbits (*Oryctolagus cuniculus*) with a mean age of 6 months and weighing between 2 and 3.5 kg were used. For the surgical procedure, the animals were sedated with midazolam (1 mg/kg) administered intramuscularly. After sedation, the animals received anesthesia with a combination of ketamine hydrochloride 10% (35 mg/kg) and xylazin hydrochloride 2% (5 mg/kg) intramuscularly. Anesthesia was maintained by the vaporization of isoflurane using a facemask. Heart rate and oxygen saturation were controlled during the transoperative period by an electrocardiogram machine.

Surgical procedure

The same surgeon performed all surgeries. Incisions were made in the proximal face of the right and left tibias, near the region of the knees, to provide access to the bone surface (tibial metaphysis). Therefore, peri-implant osseous defects (gaps) were surgically created, and the drilling of the implant sites was performed. Cup-shaped bone defects, approximately 6 mm in depth and 7 mm in width, were created with a 5-mm trephine drill and expanded with a 4-mm spherical diamond bur to characterize the peri-implant osseous defects. The apical portions of the implant sites were then prepared with a sequence of pilot, 2-mm, and 2.8-mm drills. The final measurements of the diameter of the defects were verified using a periodontal North Carolina No. 15 probe type (Hu-Friedy, Rio de Janeiro, RJ, Brazil). Then, the commercially pure titanium (grade 4) implants (Systhex, Curitiba, PR, Brazil)—with a surface treatment and measuring 3.3 $\times$ 8.5 mm, were placed into the implant drilled sites (Figure 1). They were inserted on the internal surfaces of the right and left tibias (1 implant per tibia). Following block randomization, the defects around the implants were assigned to 1 of 3 groups: group C (or negative control), in which the defect was filled with a blood clot; group AT, in which the defect was filled with a nonprocessed adipose tissue graft; and group AB, in which the defect was filled with autogenous bone graft.

For group AB, the bone was harvested with a 5-mm trephine drill in the same tibia and at the same moment as the preparation of peri-implant osseous defects around the implant sites. In addition, extra bone fragments were obtained near the peri-implant defect area with a minimum distance of 5 mm. A total of 3 bone chips were harvested for each AB experimental site. The autogenous bone was then crushed using a manual bone mill and immediately placed in the peri-implant osseous defects around the implants.

For group AT, the adipose tissue was harvested from the backs of the animals, approximately 10 cm posterior to the skull base (Figure 2). The adipose tissue was carefully removed and cut into smaller portions. Then the adipose tissue was immediately placed, without any processing methods, into the peri-implant osseous defects around the implants (Figure 3).

For group C, the formation of blood clots was expected inside the gaps. For groups AB and AT, saline-moisturized bovine collagen membranes (Genius-Baumer, Mogi Mirim, SP, Brazil) were placed to stabilize the graft materials. The membranes were stabilized with X-shaped sutures using 5.0 resorbable Vicryl sutures.

All surgical sites were sutured in 2 planes using 5.0 resorbable Vicryl sutures. For the first plane (muscle tissue of the right and left tibia), the interrupted suture technique was performed. For the second plane (dermis and epidermis of the right and left tibia), continuous sutures were used. All of the regions operated on were protected with a dressing of gauze and adhesive tape.

After the surgical procedures, the animals received, in a single application, 0.5 mL of broad-spectrum antibiotic and were administered butorphanol tartarate, 8 mg/kg, for the control of postoperative pain for 2 days.

Specimen harvesting and processing

Ninety days postsurgery, the animals were euthanized with an application of xylazine hydrochloride and ketamine hydrochloride (1 mL each) via

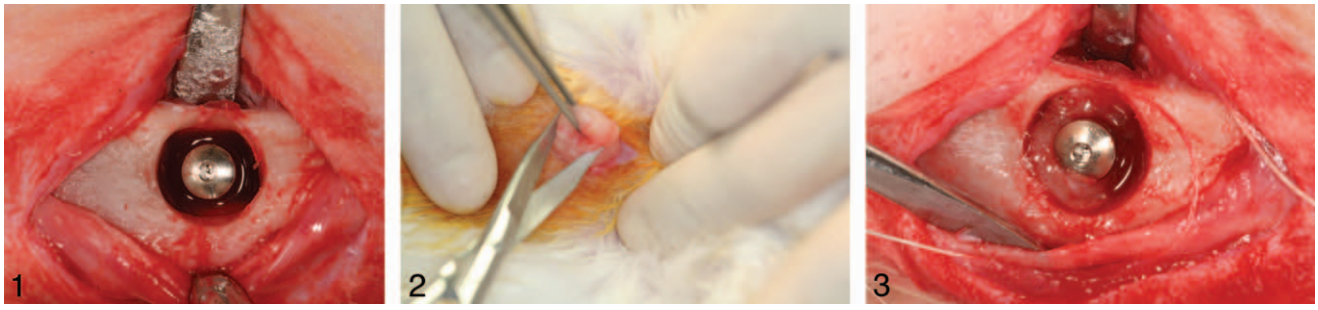

Figures 1–3. Figure 1. Implant placed in position and surrounded by the bone defect. **Figure 2.** Harvesting fat tissue with surgical scissors and forceps from the dorsum of the rabbit near to the base of the skull. **Figure 3.** Adipose tissue being placed inside the gap around the implant.

intramuscular injection, followed by an intravenous administration of 10 mL of sodium thiopental. The blocks containing the implants and the surrounding area, from the right and left tibiae of each animal, were harvested using diamond discs and fixed in 10% neutral formalin.

After fixation, the block sections were dehydrated in a series of alcohol baths and then immersed in acetone for 12 hours. After that, they were immersed in a mixture of acetone and methyl methacrylate (1:1 ratio) for 12 more hours. Next, the block sections were immersed in only methyl methacrylate for 12 more hours and embedded in acrylic resin.

To soak the block sections into acrylic resin, each one was placed in an individual test tube and then embedded with methyl methacrylate combined with 2% benzoyl peroxide (2 g of benzoyl peroxide for every 100 mL of methyl methacrylate). To avoid bubble formation, all tubes were placed in a desiccator and kept in a vacuum for 15 minutes. All tubes were then placed in an incubator at 37°C until the polymerization of the acrylic resin was complete.

Each acrylated block was sectioned using a cutting machine (Policorte Mesotom Panambra/Struers, São Paulo, SP, Brazil) and grounded/polished using a polishing table (PD-10 Panambra/Struers) until reaching a thickness of 0.20 to 0.67 mm. The thickness was measured with a digital paquimeter. One section representing the central part of the implant was prepared for each block in the mesiodistal plane and parallel with the long axis of the implant. Then the specimens were stained with toluidine blue for analysis by light microscopy.

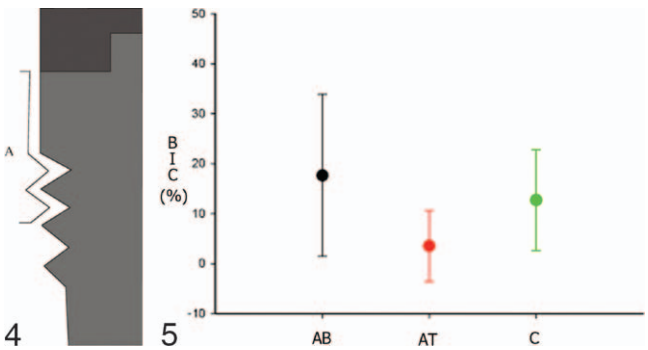

Figures 4 and 5. Figure 4. Schematic illustration of the linear measurement of bone-to-implant contact (BIC). The contact between bone and implant was measured linearly from the most coronal part of the implant until the end of the second thread (on both sides of each implant). The letter A represents this linear measurement. **Figure 5.** Scatter plot chart showing the average distribution of samples per group for BIC, with the appropriate standard deviations.

Histological and histomorphometric analyses

The specimens prepared for histological analysis were visualized in an optical microscope (Olympus BX41 TF, Tokyo, Japan) at ×40 augmentation. A camera attached to the microscope obtained the microphotographs used for the histometric analysis (Cool Snap-Pro, Media Cybernetics, Bethesda, Md). The images were obtained using the Image-Pro Plus program (Media Cybernetics, Bethesda). Images were obtained from both sides of each implant (the right and left sides). Measurements were made using image analysis software (Image Tool 3.0 [It]–UTHSCSA, San Antonio, Calif). The same investigator made all measurements. The investigator underwent a rigorous initial calibration process.

The following linear measurement was made for the histomorphometric analysis: the percentage of bone-to-implant contact (BIC), from the coronal portion of the implants on both sides (determined

Table

Mean percentage of bone-to-implant contact

	Group		
	AB	AT	C
BIC (%)*	17.64 ± 16.22	3.54 ± 7.08	12.70 ± 10.11

*Analysis of variance ($P = .25$).

by the beginning of the cover screw) to the end of the second thread (Figure 4).

Statistical analysis

Mean values and standard deviations were calculated for both sides of each implant. The data were subjected to a statistical analysis. The 1-way analysis of variance (ANOVA) test ($P \leq .05$) was performed to compare the results presented by groups C, AT, and AB in accordance with BIC. Then a post hoc Tukey HSD for multiple comparisons test was applied.

Results

Three animals died during the experimental period: 2 (group C), 1 (group AB), and 3 (group AT) specimens.

During the experimental period and sample preparation, a total of 15 specimens were discarded because of animal death or a problem with the sample preparation. The total loss of specimens was 6 in group C, 7 in group AB, and 8 in group AT.

The total specimens used for the histomorphometric and histological analysis was 6 in group C, 5 in group AB, and 4 in group AT.

Histomorphometric and statistical analyses

The linear measurements obtained from photomicrographs were converted into percentages for the comparison between groups by means of statistical analysis. The Table shows the percentage of BIC; there were no significant differences between groups ($P = .25$) after performing the ANOVA test. The distribution of the average percentage of BIC within groups is shown by graphical representation in Figure 5. The post hoc Tukey HSD multiple comparisons test showed no significant differences among groups (data not shown). In group AT, only 1 specimen presented a BIC percentage higher than 0% (specimen with 14.16%).

Histological observation

The histological evaluation for group AB showed cortical bone contact with the implant surface in 4 of 5 specimens (Figure 6). The formation of small areas of cancellous bone in contact with the implant surface was present in 2 specimens. Only 1 of the specimens did not show any cortical or cancellous bone contact within the implant surface.

For group AT, the histological examination showed that, in 3 of the 4 specimens, there was no cortical or cancellous bone contact with the implant surface (Figure 7). Only 1 sample of this group showed cortical bone in contact with the implant surface.

In group C, 5 of the 6 specimens presented cortical bone in contact with the implant surface (Figure 8). Also, 3 specimens presented medullar bone in contact with the implant surface. One sample showed no bone contact with the implant surface.

Discussion

A nonprocessing tissue technique for the use of stem cells would permit a faster approach for cell-based regeneration therapies due to the exclusion of laboratory procedures. Moreover, the costs involved in tissue-processing techniques would be eliminated. However, the results presented in group AT showed a need for tissue processing since the results were not promising. In the present study, it was observed that the experimental surgically created gaps around the implants filled with non-processed adipose tissue showed an unfavorable bone repair. After 90 days, the adipose tissue (group AT) remained clearly visible in all specimens (Figure 9). This finding differs from that found in groups AB and C, whereas bone repair seemed to occur satisfactorily. The AT group results are probably due to the lack of prior processing of the adipose tissue through enzymatic digestion, followed by

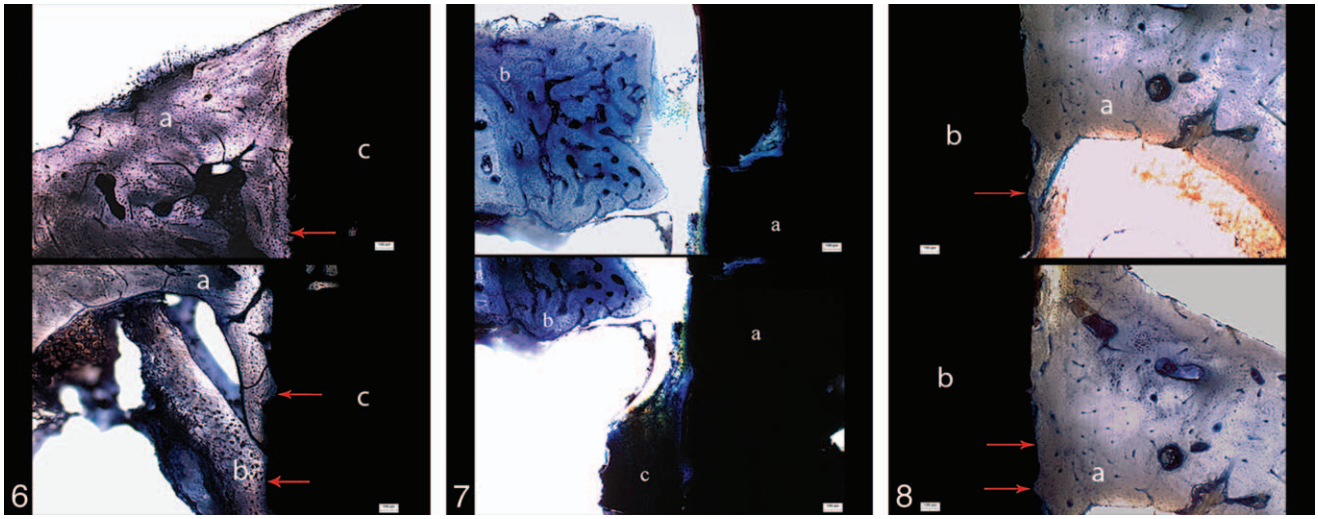

Figures 6–8. Figure 6. Photomicrographs representative of group AB showing the cortical and cancellous bone contact with the implant surface (red arrows). The letters a, b, and c represent, respectively, the cortical bone, cancellous bone, and the implant. **Figure 7.** Photomicrographs of group AT demonstrating the lack of cortical or cancellous bone in contact with the implant surface. The letters a, b, and c represent, respectively, the implant, the cortical bone, and the bone marrow bone. **Figure 8.** Photomicrographs representing group C showing the cortical bone in contact with the implant surface (red arrows). The letters a and b represent the cortical bone and the implant, respectively.

centrifugation and the collection of the pellet, which contains stem cells that are spread all around and not included in structured tissue. Such a processing method could allow the presence of approximately 2.5×10^5 available stem cells present in the pellet, free of adult fat cells contaminating the sample.[8] Thus, stem cells could be cultured for subsequent placement in the bone defect. The organized tissue seemed to prevent the stem cells from migrating toward the resident bone and then contribute to the bone repair. However, the adipose tissue was used as an experimental model because the presence of stem cells derived from adipose tissue presents, in vitro and in vivo, the ability to differentiate into osteoblasts as well as the ability of adipose cells in vitro to transdifferentiate into osteoblasts.[5,7,9] Nevertheless, these capacities did not appear to happen in our present study.

Figure 9. Group AT photograph showing a removed part of the rabbit's tibia, prior to histological processing.

Bone-to-implant contact

The results of this experiment indicate that no statistically significant differences were found between groups for BIC, ranging from 3.54% to 17.64% for groups AT and AB, respectively. These results differ from other studies with bone defects (gaps) similar to those used in our study, especially for groups AB and C.[10–15] Group AT presented only 1 specimen with bone contact, coming from the apical cortical bone and not from the bone repair of the gap. On the other hand, even accounting for only groups AB and C, Arnez,[14] after 12 weeks of an experimental period involving dogs, found in gaps of 1.5 mm in width and 5 mm in depth an average BIC for all groups of 31.84% for defects treated with autogenous bone, the protein Latex, and the control (blood clot), with no significant differences between groups. In our study, the lack of statistically significant differences between groups was probably due to the low number of specimens.

The differences found in groups AB and C may also be explained by the animal model used. The

rabbit's tibiae presented a region of marrow bone occupying two-thirds of the bone area, making this portion an empty space with respect to the presence of mineralized bone. A dense Harvesian bone cortex characterized the remaining portion. The cortical bone, when repaired in most specimens of groups AB and C, covered the implant cover screws. Most of the contact between bone and implant took place in the cover screws, which were not included in the histomorphometric measurement. A possible solution to the problem would be to use longer implants, 10 mm in length, to allow a more externalized coronal portion of the implant during placement. Another possible solution would be to replace the animal model due to the characteristics of the tibial bone of rabbits. Other animal models may provide a skeletal structure with characteristics similar to those found in humans, such as dogs, pigs, and sheep.[16] Moreover, most studies have used dogs as animal models.[1,17–21]

Bone structure

The histological evaluation of all specimens showed that 4 specimens from group AB, 5 specimens from group C, and 1 specimen from group AT presented a mature and dense cortical bone with intense Harvesian structures (osteons) and a region of abundant bone marrow. Small portions of cancellous bone were presented in contact with the implant surface in 2 specimens of group AB, in 2 of group C, and in 1 of group AT. This bone pattern is similar to that found in the study presented by Carlsson et al.[22] This same bone pattern differs from that found in other studies, including those performed in larger animals such as dogs.[19,20,23–25] The differences in the characteristics of the repaired bone formed around the implants between this study and others, performed in dogs, are due to the different macro- and microstructures of the bone in the different animal models.

An important point to be noted in our study is the fact that a bovine collagen membrane was not used in group C. The membranes used in groups AB and AT were addressed to keep the grafts in position, which was not necessary for group C, in which the bone defects were filled with blood clots. It has been demonstrated in this study that the use of membranes in group C was not necessary in light of the results presented, similar to those from group AB. This is justified because, in group AB, the material used was an autologous bone graft, which is considered the gold standard biomaterial for bone-grafting procedures.[26] Still, the fact that our study design used self-contained bone defects corroborates that claim. This assertion is supported by the study of Botticelli et al,[1] in which bone repair was tested in gaps 1-mm and 1.25-mm wide by 5-mm deep covered, or not, with bovine collagen membranes. The results of this study showed no differences in the bone repair of self-contained sites with these dimensions with and without membranes.

The results of this study demonstrate that the repair of surgically created peri-implant osseous defects in rabbit tibia was suitable for groups AB and C. Despite the lack of statistical significance between group AT and groups AB and C, the latter showed better results, as stated by the histological evaluation. Adipose tissue clearly hinders bone formation in gaps around titanium implants. Adipose tissue seems to need processing and culturing prior to application for tissue repairing and then successful use in future studies or even in a future clinical application. An in situ model of adipose tissue cell transdifferentiation could, potentially, be used to induce bone repair around implants in the future. A way to induce the migration of stem cells trapped in organized tissue toward a tissue-repair site should be investigated. Moreover, the animal model used in this study appears to be not ideal for the assessment of surgically created peri-implant osseous defects simulating gaps around immediately placed dental implants due to the micro- and macrostructural characteristics of the tibial bone of rabbits.

Abbreviations

ANOVA: analysis of variance
BIC: bone-to-implant contact

Acknowledgments

The authors thank Dr Maria Fernanda Torres, Dr Édson Alves de Campos, and Dr Adilson Yoshio Furuse for technical support. This study was supported by a grant from the Positivo University Master's Degree Program in Clinical Dentistry and by a donation of implant and membrane materials from Systhex (Curitiba, Paraná, Brazil) and Genius-

Baumer (Mogi Mirim, São Paulo, Brazil). The authors report no conflicts of interest related to this study.

References

1. Botticelli D, Berglundh T, Lindhe J. The influence of a biomaterial on the closure of a marginal hard tissue defect adjacent to implants: an experimental study in the dog. *Clin Oral Implants Res*. 2004;15:285–292.

2. Boix D, Gauthier O, Guicheux J, et al. Alveolar bone regeneration for immediate implant placement using an injectable bone substitute: an experimental study in dogs. *J Periodontol*. 2004; 75:663–671.

3. Cangini F, Cornelini R. A comparison between enamel matrix derivative and a bioabsorbable membrane to enhance healing around transmucosal immediate post-extraction implants. *J Periodontol*. 2005;76:1785–1792.

4. Gomillion CT, Burg KJL. Stem cells and adipose tissue engineering. *Biomaterials*. 2006;27:6052–6063.

5. Weinzierl K, Hemprich A, Frerich, B. Bone engineering with adipose tissue derived stromal cells. *J Oral Maxillofac Surg*. 2006;34: 466–471.

6. Qu C-Q, Zhang G-H, Zhang L-J. Osteogenic and adipogenic potential of porcine adipose mesenchymal stem cells. *In Vitro Cell Dev Biol Anim*. 2007;43:95–100.

7. Justesen J, Pedersen SB, Stenderup K, Kassem M. Subcutaneous adipocytes can differentiate into bone-forming cells in vitro and in vivo. *Tissue Eng*. 2004;10:381–391.

8. Zuk AP, Zhu M, Mizuno H, Huang J, Futrell JW, Katz AJ, et al. Multilineage cells from human adipose tissue: implications for cell-based therapies. *Tissue Eng*. 2001;7:211–226.

9. Di Bella C, Farlie P, Penington AJ. Bone regeneration in a rabbit critical-sized skull defect using autologous adipose-derived cells. *Tissue Eng Part A*. 2008;14:483–489.

10. Botticelli D, Berglundh T, Buser D, Lindhe J. The jumping distance revisited: an experimental study in the dog. *Clin Oral Implants Res*. 2003;14:35–42.

11. Botticelli D, Berglundh T, Buser D, Lindhe J. Appositional bone formation in marginal defects at implants: an experimental study in the dog. *Clin Oral Implants Res*. 2003;14:1–9.

12. Cardaropoli G, Araújo M, Hayacibara R, Sukekava F, Lindhe J. Healing of extraction sockets and surgically produced—augmented and non-augmented—defects in the alveolar ridge: an experimental study in the dog. *J Clin Periodontol*. 2005;32:435–440.

13. Botticelli D, Berglundh T, Persson LG, Lindhe J. Bone regeneration at implants with turned or rough surfaces in self-contained defects: an experimental study in the dog. *J Clin Periodontol*. 2005;32:448–455.

14. Arnez MFM. Implant's osseointegration in circumferential defects using angiogenic proteins purified from latex, autogenous bone and guided bone regeneration [thesis, in Portuguese]. Riberâo Preto, SP, Brazil: Faculty of Dentistry of Riberão Preto-University of São Paulo; 2008.

15. Yoon H-C, Choi J-Y, Jung U-W, et al. Effects of different depths of gap on healing of surgically created coronal defects around implants in dogs: a pilot study. *J Periodontol*. 2008;79:355–361.

16. Pearce AI, Richards RG, Milz S, Schneider E, Pearce SG. Animal models for implant research in bone: a review. *Eur Cell Mater*. 2007;2(13):1–10.

17. Berglundh T, Abrahamsson I, Lang NP, Lindhe J. De novo alveolar bone formation adjacent to endosseous implants: a model study in the dog. *Clin Oral Implants Res*. 2003;14:251–262.

18. Botticelli D, Berglundh, T, Lindhe J. Resolution of bone defects of varying dimension and configuration in the marginal portion of the peri-implant bone: an experimental study in the dog. *J Clin Periodontol*. 2004;31:309–317.

19. Araújo MG, Sukekava F, Wennström JL, Lindhe J. Ridge alterations following implant placement in fresh extraction sockets: an experimental study in the dog. *J Clin Periodontol*. 2005;32:645–652.

20. Botticelli D, Persson LG, Lindhe J, Berglundh T. Bone tissue formation adjacent to implants placed in fresh extraction sockets: an experimental study in dogs. *Clin Oral Implants Res*. 2006;17:351–358.

21. Jung U-W, Kim C-S, Choi S-H, Cho K-S, Inoue T, Kim CK. Healing of surgically created circumferential gap around non-submerged-type implants in dogs: a histomorphometric study. *Clin Oral Implants Res*. 2007;18:171–178.

22. Carlsson L, Röstlund T, Albrektsson B, Albrektsson T. Implant fixation improved by close fit. Cylindrical implant—bone interface studied in rabbits. *Acta Orthop Scand*. 1988;59:272–275.

23. Scipioni A, Bruschi GB, Giargia M, Berglundh T, Lindhe J. Healing at implants with and without primary bone contact. *Clin Oral Implants Res*. 1997;8:39–47.

24. Araújo MG, Sukekava F, Wennström JL, Lindhe J. Tissue modeling following implant placement in fresh extraction sockets. *Clin Oral Implants Res*. 2006;17:615–624.

25. Ito K, Yamada Y, Naiki T, Ueda M. Simultaneous implant placement and bone regeneration around dental implants using tissue-engineered bone with fibrin glue, mesenchymal stem cells and platelet-rich plasma. *Clin Oral Implants Res*. 2006;17:579–586.

26. Rawashdeh MA, Telfah H. Secondary alveolar bone grafting: the dilemma of donor site selection and morbidity. *Br J Oral Maxillofac Surg*. 2008;46:665–670.